Fast reaction products from the oxidation of CO on Pt(111): Angular and velocity distributions of the CO_2 product molecules

K.-H. Allers, H. Pfnür, P. Feulner, and D. Menzel

Citation: The Journal of Chemical Physics **100**, 3985 (1994);
View online: https://doi.org/10.1063/1.466332
View Table of Contents: http://aip.scitation.org/toc/jcp/100/5
Published by the American Institute of Physics

Articles you may be interested in

A molecular beam study of the catalytic oxidation of CO on a Pt(111) surface
The Journal of Chemical Physics **73**, 5862 (1980); 10.1063/1.440029

Kinetics of the CO oxidation reaction on Pt(111) studied by in situ high-resolution x-ray photoelectron spectroscopy
The Journal of Chemical Physics **120**, 7113 (2004); 10.1063/1.1669378

A molecular beam investigation of the catalytic oxidation of CO on Pd (111)
The Journal of Chemical Physics **69**, 1267 (1978); 10.1063/1.436666

Carbon monoxide oxidation on the Pt(111) surface: Temperature programmed reaction of coadsorbed atomic oxygen and carbon monoxide
The Journal of Chemical Physics **78**, 963 (1983); 10.1063/1.444801

Thermal excitation of oxygen species as a trigger for the CO oxidation on Pt(111)
The Journal of Chemical Physics **103**, 3220 (1995); 10.1063/1.470254

CO chemisorption on TiO_2(110): Oxygen vacancy site influence on CO adsorption
The Journal of Chemical Physics **103**, 9438 (1995); 10.1063/1.470005

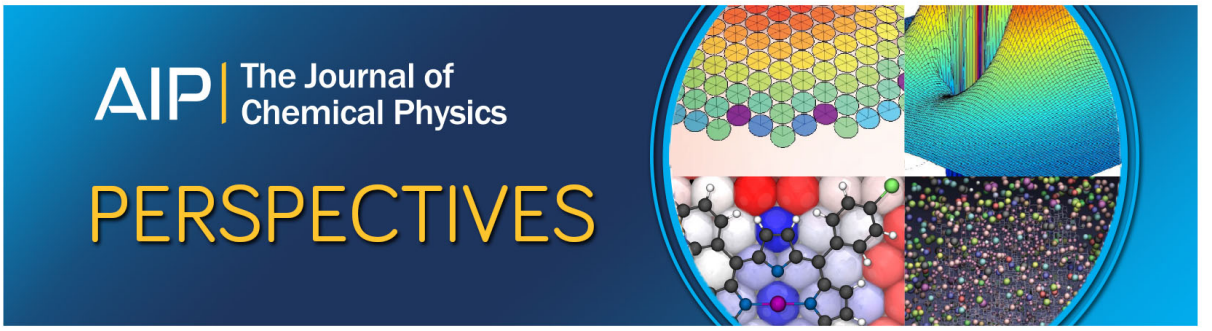

Fast reaction products from the oxidation of CO on Pt(111): Angular and velocity distributions of the CO_2 product molecules

K.-H. Allers, H. Pfnür,[a] P. Feulner, and D. Menzel
Physikdepartment E20, Technische Universität München, James Franck Strasse, 85747 Garching, Germany

(Received 6 August 1993; accepted 24 November 1993)

Angular and velocity distributions of CO_2 desorbing as reaction product of CO oxidation on Pt(111) were measured during heating of layers of initially molecular oxygen and CO adsorbed at a surface temperature of 100 K. In the velocity integrated desorption spectra of the reaction product CO_2 four different peaks (α, β_3, β_2, β_1) can be discriminated which, for linear heating rates of 5 K/s, appear at 145, 210, 250, and 330 K, respectively. They can be attributed to different reaction mechanisms which depend on the binding conditions of oxygen and the geometric arrangement and coverages of both species. Whereas α-CO_2 coincides with the O_2 desorption from and the dissociation of pure chemisorbed molecular oxygen, and thus indicates a reaction channel coupled with desorption and dissociation of O_2, β_1-CO_2 corresponds to the reaction path investigated before by many researchers and is most likely due to the reaction at the boundaries of ordered CO and oxygen islands. The structural conditions for β_3 and β_2 are less clear, but we believe them to stem from reactions in mixed and/or partly mixed layers at high coverages of O and CO. The α-CO_2 species is most likely due to reaction of CO with O atoms stemming from O_2 dissociation which react before becoming accommodated. The velocity distributions of α, β_2, and β_3 are far from thermal equilibrium with the surface as indicated by average kinetic energies between 220 and 360 meV, corresponding to $\simeq 10$ (for β_3 and β_2) and $\simeq 30$ kT_s (for α), normalized speed ratios between 0.6 and 0.8, and strongly peaked angular distributions ($\sim \cos^n \vartheta$, $n=8$ for α, $n>10$ for β_3 and β_2). For β_1 both the angular and velocity distributions show bimodal behavior with one channel fully accommodated to the surface whereas the other contains again an appreciable amount of reaction energy as kinetic energy ($\langle E \rangle \simeq 330$ meV) resulting in a strongly peaked angular distribution with $n \simeq 9$. Some TOF results for steady state reaction at high temperatures (420–800 K) obtained in the same apparatus are given for comparison. The fraction of reaction energy channelled into the translational degree of freedom for the nonequilibrated part of reaction peak β_1 is estimated to about 40%. A discussion of the various possible mechanisms is given.

I. INTRODUCTION

The oxidation of CO is one of the prototype reactions of surface chemistry and has been investigated extensively on the close packed (111) surfaces of the transition metals Rh, Pd, and Pt since Langmuir.[1] At medium to high temperatures (i.e., above 300 K), the reaction is activated, and there is universal agreement that it takes place via a Langmuir–Hinshelwood mechanism[2] on these close packed metal surfaces. The activation energy explicitly depends on the coverages of both CO and oxygen.[2–6] Detailed overall reaction schemes were established which were able to explain all essential experimental findings (such as site blocking by high CO coverages, role of islanding and diffusion) and to clarify the reaction mechanisms from a chemical point of view.[1]

The reaction dynamics, however, i.e., the distribution of reaction energy among the various degrees of freedom and their dependence on coverage and on geometric configuration of the reactands, is much less clear, even though it has also been investigated in considerable detail. For the temperature regime above 300 K, where the reaction takes place between adsorbed CO and O adatoms, already the earliest molecular beam investigations on evaporated Pt films[7] reported strongly peaked angular distributions of the CO_2 product, and the earliest time-of-flight measurements on Pt(111)[8] detected very fast CO_2 molecules whose kinetic energy depended on the polar angle; this was also found later on Rh(111).[5] Later angular distribution measurements on Pt(111), with molecular beams[2,9] as well as during reactive thermal desorption (RTPD)[10] yielded results which showed bimodal behavior (superpositions of $\cos \vartheta$ and $\cos^n \vartheta$ behavior) for certain conditions, which the earlier measurements had not resolved. The earlier work on velocity distributions, carried out at very low coverages,[5,8] did not resolve a bimodality in the kinetic energy distributions (which one would expect from the angular results). Very recent molecular beam measurements, however, did report a bimodal velocity distribution for CO and O coverages less than 0.1.[11] Also, very recently, the first work apppeared on combined measurements of angular and velocity distributions in thermal desorption.[12] It deals with CO oxidation on Pd(110) and Pt(110) showing special effects due to the geometrical structure of these surfaces. These very recent works[11,12] parallelled our investi-

[a]Now at Institut für Festkörperphysik, Universität Hannover, Appelstrasse 2, 30167 Hannover, Germany.

 0021-9606/94/100(5)/3985/14/$6.00 © 1994 American Institute of Physics

gations. As to the internal degrees of freedom, there are data on the vibrational and rotational distributions of the product molecules[13,14] which may in part contain collisional and contamination effects due to the moderate vacuum conditions and the surfaces (Pt gauze and foil) used for these chemoluminescence measurements but can certainly be taken as correct in the main conclusions; they show strong heating for both rotations and vibrations, the latter with some preference for particular modes.

Starting with coadsorbate layers of CO and molecular O_2, Matsushima[10] had discovered a second channel of CO_2 production which parallels the desorption and dissociation of O_2. Rettner *et al.*[15] used this reaction to probe for molecular vs atomic adsorption of oxygen and found[16] that atomic oxygen brought in from the gas phase reacted with CO, with the resulting CO_2 again being very fast and strongly peaked in the surface normal. Mieher and Ho[17] showed that the reaction between coadsorbed O_2 and CO can also be stimulated by photoexcitation.

We have used our recently developed method for angularly resolved velocity distributions of thermally desorbing molecules[18] to investigate these properties for reactively desorbing CO_2 liberated from layers of coadsorbed CO and O_2 on Pt(111) during heating with a linear temperature ramp. Although this method only gives access to the translational degree of freedom and to its angular distribution, it has the advantage over molecular beam methods that also the high coverage regime can be investigated with ease. We find that due to the high density of the adsorbed layers additional reaction channels open up. These reactions proceed between 145 and 330 K. Some complementary results for steady state CO_2 production at 420 to 800 K are also reported. Apart from the thermal contribution in a bimodal peak, all separable states are strongly hyperthermal in translational energy; the flux of desorbed CO_2 is strongly peaked around the surface normal. These results extend the available information; where overlap with other work exists, the agreement is usually good. We use our interpretation of these results for a qualitative and partly tentative discussion of the mechanisms involved which should stimulate further, in particular theoretical work.

II. EXPERIMENT

The experimental setup and the procedures of data evaluation have been described in more detail in Refs. 18 and 19. Therefore, we only give a short summary. The experimental equipment consists of a double chamber UHV system. One chamber (base pressure 2×10^{-11} mbar) is equipped with the sample manipulator, a retarding field LEED/Auger system, sputter gun, the gas doser, and a chopper motor. The second chamber contains the time of flight (TOF) tube (length 380 mm) with mass spectrometer detector and is separately pumped. The walls of the TOF tube are used as pumps by evaporating a Ti film onto them. The tube together with the entrance slits was lN_2 cooled which led to an effective pumping speed of at least 4000 ℓ/s for CO. A 30 ℓ/s ion getter pump was added to this chamber as a holding pump. In a second version the Ti getter was replaced by a layer of activated carbon pasted onto the cryoshield.[20] This increased the pumping speed by about 1 order of magnitude.

The sample was cut from a 99.999% pure Pt single crystal rod, oriented to better than 0.2° and polished with diamond pastes down to 0.25 μm grain size. For mounting Ta wires of 0.5 mm diameter were spot welded to the back side of the samples and were directly used for resistive heating. Sample temperatures were measured by chromel–alumel thermocouples also spot welded to the samples and controlled by a microcomputer.[21] Cleaning was accomplished by heating cycles up to 900 K in 1×10^{-6} mbar of oxygen. Thick layers of carbon on the new sample were removed by sputtering and annealing to 1400 K. Tests for cleanliness were done routinely by Auger spectroscopy.

A chopper blade (125 mm diameter) with four slits (rectangular shape, 3.8×10 mm) mounted on a three phase chopper motor inside the main chamber was used to provide the time base for the TOF experiments. The rotation frequency was continuously adjustable between 30 and 100 Hz. The angular resolution is estimated to be 2°–3°. Normal TPD spectra at certain polar angles were carried out with the slit open permanently. To measure translational energies, the chopper was run during TPD, and TOF spectra were recorded continuously. Temperature intervals corresponding to certain TPD peaks could be selected from these data.

TOF signals were recorded using a multichannel scaler (MCS) with up to 2048 channels. The measuring time per channel was adjustable with a resolution of 0.1 μs. Up to 65 535 scans could be accumulated. Each scan was started by a new trigger pulse.

As described in Ref. 18, the ideal TOF spectrum, $f(t)$, is in general experimentally broadened by a convolution with the chopper opening function, by the finite length of the ionizer of the mass spectrometer and by the finite time interval per channel of the MCS, and further modified by the velocity dependence of the ionization probability, w. All these influences on the experimentally measured TOF spectra have been carefully measured individually. The mass spectrometer turned out to work as an ideal density detector ($w\sim1/v$). The chopper opening function, P, is given by geometry and has trapezoidal form.

The dominating uncertainty in the TOF spectra is due to the determination of the trigger delay, i.e., of the starting point in time of the TOF spectra. Therefore, calibrations were carried out either using a beam with Maxwellian distribution and known temperature, or detecting the light from the ion source emitted through the chopper slit with a photodiode. By systematic calibration it was possible to reduce the uncertainty to ±1 channel.

TOF distributions were determined by fits to the experimental curves assuming a known distribution $f(v)$ as fit function with the experimental parameters as determined above. As a fit function for $f(v)$ the form

$$f(v)=v^3\exp\left[-\frac{m(v-v_0)^2}{2kT}\right] \tag{1}$$

was used. By variation of T and v_0 the average kinetic

energy $\langle E \rangle$ and the width (expressed as speed ratio, SR, see Ref. 18) can be varied independently. For a Maxwellian beam in equilibrium with the surface $v_0=0$ and $T=T_s$ (where T_s is the sample temperature); the given SR values are normalized to the Maxwellian value.

For gas dosing a capillary array was used in order to avoid heavy gas loads in the chamber. All layers in these experiments were prepared at a surface temperature of 100 K by *first* dosing the exposures of oxygen and then of CO. At this surface temperature no reaction occurs. The oxygen layers at this temperature are in a *molecular* chemisorbed state.[15,22,23] Upon heating they partly desorb and dissociate and, if CO is coadsorbed, react to form CO_2.

III. RESULTS

A. Energy integrated reactive thermal desorption

In order to characterize the oxidation reaction during thermal desorption starting from high oxygen and CO coverages and to compare with data published in the literature for smaller coverages[3,10] an overview of the reactive programmed thermal desorption (RTPD) spectra of CO_2 as function of increasing oxygen and CO exposures for normal emission ($\vartheta=0°$) is shown in Fig. 1. The surfaces were heated using a linear heating rate of 5 K/s unless indicated otherwise, and the CO_2 signal was recorded during reaction. Possible simultaneous desorption of O_2 and CO was not investigated. However, relative amounts of oxygen remaining on the surface after completion of the reaction and complete desorption of CO (Ref. 3) were measured by desorbing it at temperatures above 600 K.

For calibration purposes, layers of *atomic* oxygen were produced first by dosing various amounts of oxygen gas at a surface temperature of 100 K and subsequent heating to 200 K. Subsequently, a constant exposure of 2.7×10^{15}/cm^2 of CO was dosed. The product spectra of CO_2 show a peak at 330 K (β_1) and a small shoulder (β_2) at 250 K; the main reaction peak shifts slightly to higher temperatures with increasing coverages of atomic oxygen. Atomic oxygen layers produced as just described saturate at a coverage of Θ_O of 0.25, and produce a sharp $p(2\times2)$ LEED pattern.[3,23] The reaction spectrum corresponding to this condition is shown in Fig. 1 as curve a which agrees very well with the data of Ref. 3. From the data of Ref. 3 one can conclude that only 1%–15% of the original coverage of atomic oxygen does not react with CO under the conditions used here. This spectrum was used for calibration, therefore, and the product yield (i.e., CO_2 molecules produced per Pt surface atom) set to 0.22.

The reaction gets considerably more complicated when we start with coadsorbed molecular oxygen and CO, formed at $T_s=100$ K, as shown in spectra *b* to *k* of Fig. 1. The three columns of spectra correspond to three different exposures of CO. The oxygen exposure was varied, as indicated. In addition to the β_1 and β_2 peaks just mentioned, two more peaks at 145 K (α) and around 200 K (β_3) appear, depending on initial coverages mainly of oxygen. For runs b, c, and d no atomic oxygen was found to be left on the surface after reaction and desorption of CO.

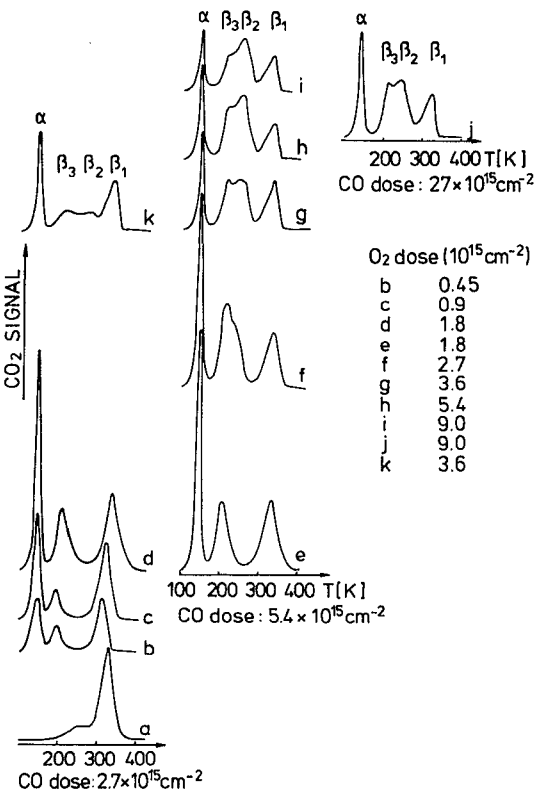

FIG. 1. Overview of thermal desorption spectra of CO_2 after reaction of oxygen and CO. Four desorption peaks (α, β_3, β_2, and β_1) can be discriminated. Layers of O_2 and of CO were dosed in this order successively at 100 K (exception: curve a, which served as reference spectrum with $\Theta_O=0.25$, see the text). The three columns correspond to the three different CO exposures indicated. The oxygen exposures (given in insert on the right) increase from bottom to top of the drawing. Heating rate: 5 K/s.

Whereas the α-CO_2 peak stays at a constant desorption temperature, the β_3 and β_1 peaks shift towards higher desorption temperatures with increasing doses of oxygen.

For the spectra in the center column of Fig. 1 the CO exposure was twice that for the left column. This has little effect on the reaction yield and the thermal desorption spectrum of CO_2 at medium pre-exposures of oxygen (compare runs d and e in Fig. 1; no O was left after reaction for e and f), but a fourth peak is coming up around 250 K (β_2) with increasing oxygen exposure. This peak appears at the same desorption temperature as the shoulder of curve a which was produced by reaction of CO with a saturated layer of atomic oxygen (see above). A comparison of the other runs with this spectrum shows that the position of peak β_1 is only affected slightly by varying the amounts of adsorbed CO and oxygen. Starting at spectrum g a reduction of CO exposure back to the value of the left column only affects peaks β_2 and β_3, the integral of which is cut half, but leaves the other peaks unchanged (spectrum k). A fivefold increase of CO exposure at high oxygen coverages, on the other hand, has very little effect on the product yield (see Table I) and the distribution between desorption peaks (compare runs i and j).

TABLE I. Absolute values of product efficiency for the different desorption spectra shown in Fig. 1. A product yield of one means the production of one CO_2 molecule per Pt atom. Run a was used for calibration (see also Ref. 3. For details, see the text).

Spectrum	O_2 exposure $10^{15}/cm^2$	Initial O_2 coverage	CO exposure $10^{15}/cm^2$	Product yield α	β_3	β_2	β_1	Σ
a	$p(2\times2)O$		2.7	0	0	0.03	0.19	0.22
b	0.45	0.1	2.7	0.08	0.03	0	0.09	0.20
c	0.9	0.3	2.7	0.11	0.06	0	0.15	0.32
d	1.8	0.43	2.7	0.19	0.12	0	0.16	0.47
e	1.8	0.43	5.4	0.20	0.14	0	0.16	0.50
f	2.7	0.47	5.4	0.15	0.17	0.07	0.13	0.52
g	3.6	0.48	5.4	0.09	0.08	0.11	0.10	0.38
h	5.4	0.49	5.4	0.08	0.09	0.12	0.07	0.36
i	9.0	0.50	5.4	0.06	0.06	0.09	0.07	0.30
j	9.0	0.50	27	0.10	0.11	0.09	0.08	0.38
k	3.6	0.48	2.7	0.09	0.03	0.04	0.10	0.26

Although our data were partially taken under conditions different from those published in the literature[3,10,15] and extend to higher coverages, an identification of the reaction of molecular and of dissociated oxygen with CO is possible by comparison. There is no question that peaks β_1 and β_2 are due to reaction of *atomic* oxygen with CO. As to the α peak, Matsushima[10] who saw this peak first, showed with isotopic marker experiments that it is due to reaction of CO with *molecularly* adsorbed oxygen; he further concluded that both oxygen atoms from a molecule are used for oxidation of two CO molecules. The fact that he only observed two peaks (our β_1 and α peaks) could be due to his different pre-coverage conditions but also to his higher adsorption temperature of 125 K where the reaction already starts. (The discrepancies between these and our results are not due to slow kinetics, as we obtained identical results by varying the heating rate between 2 and 20 K/s.) Desorption and dissociation of molecular oxygen in pure layers occurs around 150 K,[24] i.e., at the same temperatures where the α peak is found, and is completed below 160 K. Coadsorption of CO is not expected to stabilize the O_2 bond so that no molecular oxygen should exist above 160 K in mixed layers either. We have carried out a direct comparison of the α CO_2 peak with the desorption peak of molecular O_2 from pure O_2 layers on Pt(111), on the same surface and in the same apparatus,[23] and found complete agreement of the two peaks. Results very similar to ours, but with no systematic variation of coverages, were obtained by Rettner *et al.*[15] From their experiments using partially dissociated oxygen beams and from our direct comparison it is clear that *all three* β peaks (which they found at the same temperatures as we did) are due to reaction of *dissociated* oxygen with CO. The origin of the three peaks will be discussed below.

In order to get more quantitative insight into the reaction mechanisms we determined the peak areas of the different reaction peaks of Fig. 1. These results are shown in Table I. Calibration of the product yields was done using again spectrum a of Fig. 1. Uncertainties in separation of the different peaks and in reproducibility are estimated to be around 5%. The different angular and velocity distributions of the various desorption peaks (see below) were not corrected for, since the differences are small for the main peaks (see below). The amounts of oxygen preadsorbed were determined explicitly in our work on O_2/Pt(111) with the same apparatus[23] using the completed $p(2\times2)$ structure of atomic oxygen as absolute reference. Unfortunately, because of technical reasons no structural information by LEED could be obtained under reaction conditions.

The following characteristic properties of the reaction were found under the conditions mentioned above: For runs b through f no remaining oxygen existed on the surface after completion of the reaction. For the conditions of spectrum b this means that the complete oxygen layer must have reacted with CO, whereas for higher oxygen precoverage the reaction probability decreases to a value around 0.55 for spectra d, e, and f. This decrease must be due to the onset of desorption of molecular oxygen which competes with dissociation and with reaction in peak α, and is not mainly due to a lack of CO, as evident from the marginal difference between curves d and e where the CO exposure was doubled, and from the complete consumption of dissociated oxygen.

Blocking of adsorption sites for CO by preadsorbed molecular oxygen only comes into play near saturation of molecular oxygen, as can be seen comparing curves g to i where the reaction probability decreases further although the initial oxygen coverage still increases slightly. Explicit measurements after runs g and h found remaining coverages of atomic oxygen of 0.06 and 0.08, respectively. This blocking of CO adsorption has a much stronger dependence on coverage of molecular oxygen than would be expected for steric reasons. Close to initial saturation with oxygen, coverage changes in the reaction kinetics are observed leading to the appearance of the β_2 peak. It grows at the expense of all other peaks, including α. As an example, a comparison of curves e and h shows an increase of total initial oxygen by about 10% and roughly constant sum of CO_2 from reaction with atomic O (sum of β peaks), but a 30% share of β_2 in the second case (compared to zero in the first) and a decrease of the other peaks by between 40% and 60%, and of the total CO_2 by one third. Thus the strong nonlinear blocking of CO adsorption by high O_2

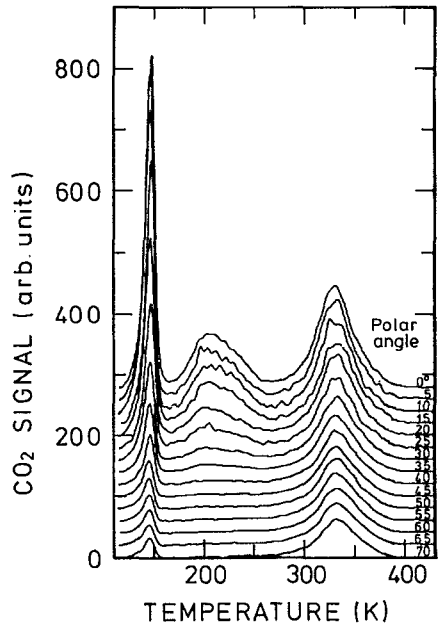

FIG. 2. Reactive temperature programmed desorption (RTPD) of CO_2 as a function of emission angle after predosing 1.5×10^{15} cm^{-2} molecules of O_2 and 2.7×10^{15} cm^{-2} molecules of CO successively at $T_s=100$ K. Heating rate 5 K/s.

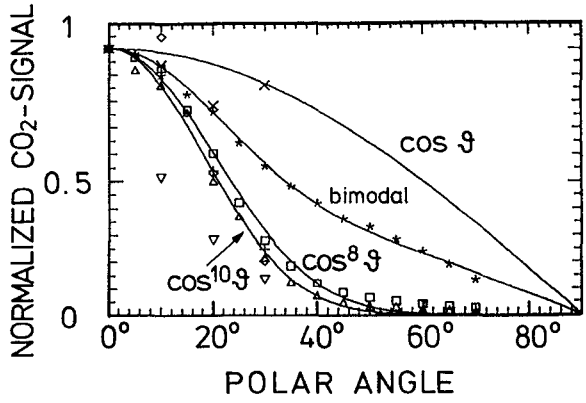

FIG. 3. Results of a quantitative evaluation of the angular dependence of desorption fluxes from Fig. 2 for desorption peaks α (□), β_2 and β_3 (△), and β_1 (*). In addition results from TOF distributions at different angles of emission are shown by different symbols: peak α (◇), β_2 and β_3 (▽), β_1^f (+) and β_1^s (×).

coverages has a complicated effect on the partitioning into the remaining channels.

It is also seen that very dense adsorbed layers can be produced by sequential coadsorption of O_2 and CO. In runs e and f a total coverage of close to one can be reached which is considerably higher than the respective saturation coverages of the pure species. This remains even valid for dissociated oxygen. O coverages up to 0.35–0.38 can be reached in these mixed layers (as seen already from the sum over the β peaks which give a lower limit), compared to a saturation coverage of only 0.25 in the pure layer of dissociated oxygen.

B. Angular and time of flight distributions

1. Angular distributions

The desorbing flux of CO_2 after reaction was found to be strongly peaked along the surface normal for all desorption peaks except for β_1, which has both a strongly peaked and a $\cos\vartheta$ contribution. An example of angularly resolved thermal desorption, obtained by integration over all kinetic energies, is shown in Fig. 2 for exposures of 1.5×10^{15} cm^{-2} of oxygen and 2.7×10^{15} cm^{-2} of CO. The quantitative evaluation is given in Fig. 3. For this purpose the spectra of Fig. 2 were divided up into three temperature intervals covering the CO_2 peaks α, β_3 plus β_2, and β_1, respectively. As it turns out that the average kinetic energy of the $\beta_{2/3}$ peaks does not vary with polar angle and the variation for the α peak and the peaked part of the β_1 peak is not strong (see below), no corrections of mass spectrometer sensitivity were necessary here. Peaks α and β_3 can be rather well described by $\cos^n\vartheta$ distributions with n between 8 and 10. Even more interesting is the bimodality of the β_1 peak. As shown in Fig. 3, its angular dependence can be quantitatively described by adding contributions from $\cos\vartheta$ and $\cos^8\vartheta$ functions where the ratio of the integrals of the two contributions (now taking the different spatial and velocity distributions into account) is about 1.5 for the conditions shown. These strongly peaked angular distributions are indicative of inefficient accommodation of the desorbing CO_2 molecules after reaction; only the cosine part of the β_1 peak seems to be able to accommodate during desorption.

2. Velocity distributions

This becomes even more clear and quantitative from the results of velocity distributions, obtained from TOF experiments and shown in Figs. 4 and 5. For these sets of experiments the subdivision into three temperature ranges was maintained as peaks β_2 and β_3 could not be uniquely separated in the TOF experiments. Somewhat different precoverages (3.6×10^{15} cm^{-2} of oxygen, 2.7×10^{15} cm^{-2} of CO, corresponding to curve k of Fig. 1), were used. The higher oxygen dose not only makes the β_2 peak more visible compared to the experiments described above. The reduction of the β_3 peak is probably due to a smaller concentration of CO as now excess oxygen is present on the surface and is also found after completion of the reaction. The residual O concentration for reaction in the β_1 peak can be estimated to be between 0.28 and 0.18. These differences in oxygen coverage compared to the velocity integrated measurements described above have only some quantitative consequences; the qualitative behavior is unchanged.

The results of the three temperature regimes are illustrated in Fig. 4 together with fits according to Eq. (1) which are seen to describe the data perfectly. The contribution of two velocity distributions to peak β_1 is as obvious as was the bimodality in the angular distributions. Because of their different dependence on polar angle they can be more clearly separated at larger polar angles, as demonstrated in Fig. 5. Quantitative evaluations of these fits show

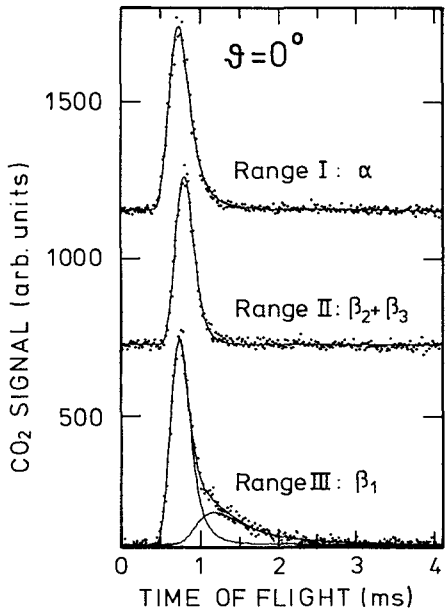

FIG. 4. TOF distributions for CO_2 during RTPD for emission normal to the surface, for the three temperature ranges corresponding to α (I), $\beta_2+\beta_3$ (II), and β_1 (III). Predose: O_2: 3.6×10^{15} cm^{-2}, CO: 2.7×10^{15} cm^{-2} at $T_s=100$ K, heating rate: 10 K/s. Lines mark fits to the data according to Eq. (1). The bimodal distribution in β_1 can clearly be seen.

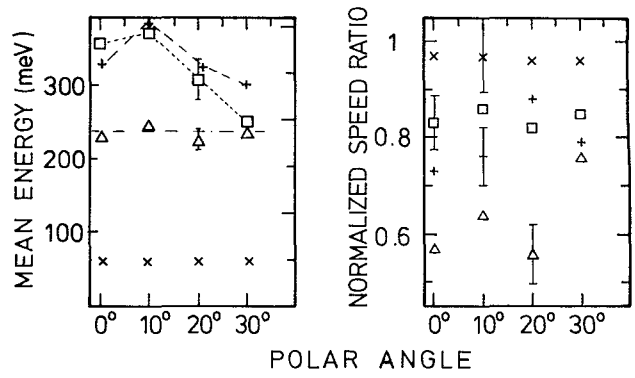

FIG. 6. (a) Average kinetic energy of desorbed CO_2 from CO oxidation in meV as a function of polar angle of emission. The different symbols mark the different desorption peaks α (□), β_2 and β_3 (△), β_1, fully accommodated part (×), β_1, fast part (+). Lines are only meant to guide the eye. (b) Normalized speed ratios for the TOF distributions evaluated in (a) as a function of polar angle of emission. Symbols used are the same as in (a).

that only the slow contribution to peak β_1 (named β_1^s hereafter; the fast component is called β_1^f) can be described by a Maxwell distribution at the surface temperature, with an average kinetic energy of $2kT_s$ [see Fig. 6(a)], where T_s is the mean surface temperature during reaction. Correspondingly, the speed ratio, SR, which is normalized to a Maxwell distribution,[19] is found to be one within error limits [Fig. 6(b)]. All other distributions deviate strongly from Maxwellians: Expressed in units of surface temperature, values around 10 are found for the nonaccommodated β peaks, and of about 30 for the α peak. Because of this clear hyperthermal behavior, the surface temperature is not a sensible unit, and Fig. 6(a) plots instead the absolute mean energies as a function of polar angle. These values do not depend on polar angle of desorption for $\beta_{2/3}$, while for peaks α and β_1^f, this is the case. This is clearest for the data of α, where there is a decrease of one third from normal emission of 30°. For β_1^f, the data are not as clear, but within the error bars they agree with those for α—which is surprising in view of the very different mechanisms expected for these peaks. Also, the speed ratios [see Fig. 6(b)] are considerably smaller than 1, ranging from 0.6 for the β_2 and β_3 peaks to 0.8 for α and β_1^f; the latter agreement makes it less likely that the similarity found for the mean energies is a coincidence. Numerical values of kinetic energies (also in units of surface temperature for demonstration) are given in Table II.

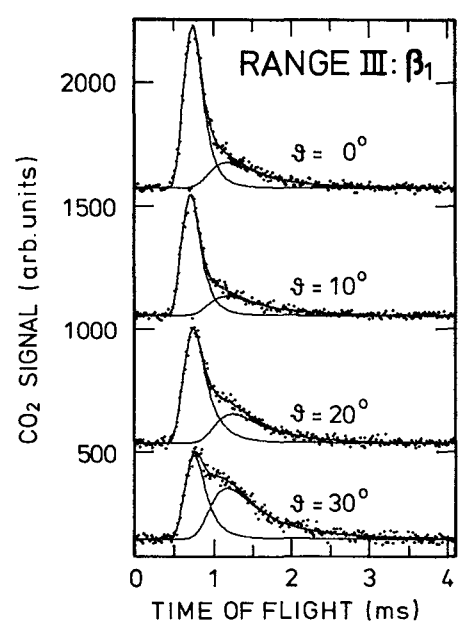

FIG. 5. Same as Fig. 4 for β_1 (region I) only, but at various angles of emission.

Consistency checks were carried out constructing velocity-integrated angular distributions from the TOF spectra taken at difficult angles. These data are included in Fig. 3; good agreement is found in most respects. Angular variations of kinetic energy were taken into account only for peak α, but this has only a small effect on the angular dependence of this peak. Again, the β_1 peak can be quantitatively resolved into the two contributions mentioned. The exponent n of the $\cos^n\vartheta$ distribution for the β_1^f peak was found to be 9 ± 2, in good agreement with the other data of Fig. 3, and the ratio of the integrals over the cosine and the peaked distributions was close to one (the slight difference to the value derived from the mere angle distributions, if outside the reproducibility, is probably caused by the higher oxygen coverage). The only large deviation of the angular dependence compared to the velocity integrated measurements was found for the combined peak β_2 and β_3, which is even more strongly peaked in the TOF

TABLE II. Values of average translational energies of CO_2 for the different reaction channels (see the text).

Energy	Reaction peak $\alpha(\vartheta=0°)$	$\alpha(\vartheta=30°)$	β_2 and β_3	β_1^f	β_1^s	Product energy $\Theta_O, \Theta_{CO}\simeq 0$	$\Theta>0.1$
(meV)	355	250	227	329	57	1448	900
(kT_s)	28.2	19.9	12.3	11.6	2.0		

experiments. This must be an effect of the different weighting of the β_2 and β_3 contributions in the two experiments. Since β_2 is weighted more strongly in the TOF data, this species must be even more strongly peaked than β_3; an estimate yields $n\geq 20$ for β_2.

TOF experiments have also been carried out at various desorption angles under continuous flow conditions of both oxygen and CO at elevated surface temperatures between 420 and 800 K. Various fluxes of CO and oxygen in the range between $1\times10^{14}/(cm^2\ s)$ and $1\times10^{15}/(cm^2\ s)$ were tested. With these fluxes only reactions corresponding to the β_1 peak (or rather its extension to lower coverages) can take place at these surface temperatures. Bimodality of both angular and velocity distributions was also found here. As a function of temperature the relative amount of the accommodated channel decreased at constant flow conditions from 16% at the maximum product yield, which appears at surface temperatures around 540 K, to the limit of detectability (i.e., below 5%) at $T_s=800$ K. For the fast reaction channel the average translational energy increased with surface temperature from 440 meV per molecule at $T_s=420$ K to 600 meV at $T_s=800$ K, whereas the speed ratio SR remained at a value around 0.75, in agreement with the RTPD measurements for β_1^f. Angular distributions were also in good agreement with those obtained during RTPD.

IV. INTERPRETATION AND DISCUSSION

A. Assignment of reaction states

The oxidation of CO on Pt(111), and on other metal surfaces of the platinum group, is generally accepted to be a reaction of the Langmuir–Hinshelwood (LH) type,[1] at least under conditions of supply of molecular CO and O_2 from the gas phase. This means that all elementary steps of this reaction take place on the surface after full accommodation of the real reactants—CO and atomic oxygen—on the surface. In our case of supply from a preadsorbed mixed layer of molecular O_2 and CO (which evolves into these reactants by heating), it might appear that there is no other possibility. However, the properties known for α CO from earlier[10,15] and the present work will lead us to the conclusion that this peak cannot be due to a LH reaction in the strict sense, since it appears to be due to reaction of not fully accommodated O atoms with adsorbed CO. We will elaborate on this below.

The β peaks are unquestionably due to reaction of adsorbed O atoms with adsorbed CO, i.e., to LH pathways. However, the temperatures necessary for measurable reaction rates are much lower for our coadsorbate layers than for supply from the gas phase. This must be due to their (partly much) higher adsorbate densities and their more favorable relative distribution; this range is not accessible to the continuous reaction conditions investigated with molecular beams[1,8] or generally gas phase supply as in our steady state reactions. We expect, therefore that effects of local ensembles (density and arrangement), order, restricted mobility and diffusional effects, part of which have been seen in the cited earlier work, are of considerable importance and contribute to the splitting into the three β peaks seen. The main difference between RTPD reactions and reaction under gas phase supply is then that for the former, initial conditions of very high densities and intimate mixing of reactants can be prepared, with consequent high reaction rates at comparatively low temperatures, while under supply from the gas phase the deviation from twodimensional equilibrium should be small, since mobility is appreciable and segregation into islands as well as order/disorder phenomena occur readily. For RTPD, temperature and coverages are then not sufficient as parameters to define the reaction rate, but the reaction probability will depend explicitly on the prehistory of the layer which will determine the local configuration on the surface, in particular at high coverages. RTPD is thus not just a slightly different method, but gives access to conditions not accessible to experiments under gas phase supply. The detailed characterization of these pathways is a specific piece of new information obtained in our experiments.

The effect of restricted surface mobility is already obvious from pure $p(2\times2)$ ordered layers of atomic oxygen on Pt(111) which turn out to be practically immobile up to a surface temperature of 500 K.[25] Unfortunately LEED observations under identical conditions are not available, so that the conclusions we can draw about structural conditions during reaction rely on analogy with CO oxidation experiments carried out on the Pd(111) surface,[26] which behaves very similarly regarding the parameters relevant here (even though the dynamics of reaction must proceed quite differently, as shown by the fact that only accommodated product molecules evolve on that surface): The binding energies for atomic oxygen on these surfaces are virtually identical[27,28] as well as those for CO.[29,30] Also the tendency of atomic oxygen for island formation already at low coverages is found on both surfaces.[3,31] For coadsorbed layers of CO and O on Pd(111) a mixture of three adsorbate structures has been suggested: islands of $p(2\times2)$ and, as a compression structure, $(\sqrt{3}\times\sqrt{3})R30°$ ordered islands of atomic oxygen in coexistence with $(\sqrt{3}\times\sqrt{3})R30°$ ordered CO, respectively. Reaction of CO and O ordered in these types of islands leads to practically identical reaction peaks.[26] As a third structure a (2×1) ordered mixed phase of O and CO has been proposed. This phase has been

shown to be extremely reactive, leading to a product peak during TPD already at 250 K.[26] We note that it is likely that the important parameter is not the order itself, but rather the local density and (de)mixing which is connected with the formation of such structures.

For the Pt(111) surface the origin of reaction peak β_1 is easiest to identify as we also found it for the well ordered $p(2\times2)$ layer of preadsorbed atomic oxygen, in agreement with Gland and Kollin.[3] These authors suggested it to originate from the reaction of mobile CO at the perimeter of ordered O islands which they found to occur under all of their coverage conditions. As oxygen has a tendency to cluster even at small oxygen coverages[3] this type of reaction can be maintained over a fairly wide range of coverages down to a very small fraction of an oxygen monolayer where islands become unstable and a lattice gas of oxygen has to be formed. The similarity of the β_1 peak in all our spectra suggests that the origin is always the same which would mean that segregation and ordering of the remaining O layer occurs at least by 300 K, since our original layers are certainly mixed. Furthermore, there seems to be agreement in the literature that the β_1 RTPD peak corresponds to a reaction path which is locally similar to that occurring at higher temperatures/lower coverages under supply from the gas phase. The remaining differences in detail, in particular concerning the observed activation energies and product translational energies, have been explained by coverage influences; this can also be done in our case (see below). We therefore also assume that β_1 is due to LH reaction between coadsorbed CO and O at the boundaries of segregated O and CO islands for dense and dilute layers, and of isolated CO and O species at high temperatures and low coverages (gas phase supply). This implies that the local O concentration for β_1 is equal or below that corresponding to the (2×2) structure. The shoulder seen in spectrum a of Fig. 1 can be interpreted in analogy with the findings on the Pd(111) surface for the mixed high density layers recalling the fact that up to 0.5 ML of CO can still be adsorbed on a surface saturated with atomic oxygen[3] (a saturated CO layer, however, completely blocks dissociation of O_2[1]). Mixed layers of O and CO must be formed by exposing the $p(2\times2)$O precovered surface to a high dose of CO at low T. As a consequence, part of the CO must react with its neighboring oxygen atoms before segregation can occur. If the analogy with the reaction on the Pd(111) surface is correct, these mixed layers are more reactive and product formation occurs at lower temperatures than for the segregated phases.

This suggested mechanism is consistent with the occurrence of the reaction peaks β_2 and β_3 at desorption temperatures considerably lower than for the β_1 peak, as the concentration of atomic oxygen on the surface after dissociation of oxygen molecules within a mixed layer of CO and O_2 is considerably higher than after exposure to pure oxygen gas at 300 K. As mentioned above, the coverage of atomic oxygen can be as high as 0.38 in a coadsorbed layer of O and CO under our measuring conditions. Furthermore, the formed O layer is likely to be disordered, and intimately mixed with CO. The β_3 peak occurs under conditions where O_2 desorption and dissociation has just been completed and the O coverage is at a maximum; the coadsorbate layer is very dense and intimately mixed (excluding the need for transport steps). This, possibly together with a decrease of activation energy due to the high coverage (see below), then leads to the high reactivity seen in β_3.

The intermediate β_2 peak occurs at the temperature of the shoulder for the $p(2\times2)$–O layer, but for very high initial O_2 and even higher remaining O coverages. It is only found for initial total (O+CO) coverages above 0.5, and grows at the expense of all other peaks. The diminution of the α and β_3 peaks under conditions of high β_2 is likely to be due to the lower CO coverage that can be postadsorbed at these high O_2 coverages: the unaccommodated O atoms produced during O_2 desorption (see below) do not find as many CO partners, and the number of CO molecules in the spatial arrangement required for the β_3 peak is also lower. The increase of the β_2 peak that follows may indicate that a transport step is necessary for it. This could possibly mean that β_2 does require some initial islanding as well; but the transport could also simply involve the CO. The β_2 shoulder found for the full $p(2\times2)$–O structure could possibly be due to reactions in regions of increased O density, e.g., at domain boundaries of the $p(2\times2)$–O structure. Similar compressed situations could form at a larger scale during incipient mobility of the still dense (O+CO) layer induced by the heating, together with provision of space by β_3 desorption. Structural information in this range would be highly desirable; but as noted order is certainly not a prerequisite.

From these considerations the following scenario of successive reaction and desorption seems to be most likely after adsorption at a surface temperature of 100 K of mixed layers of CO and molecular O_2. During heating of these coadsorbed layers three parallel reaction channels become effective between 130 and 170 K, for high O_2 coverages: desorption of O_2, making possible dissociation of O_2, which leads to direct reaction into α CO_2, leaving atomic oxygen and CO on the surface. For low O_2 coverages, dissociation can proceed without desorption. It seems to be most likely, and consistent with the argument just given, that the layer produced by these processes is essentially randomly mixed, because this reaction takes place in presence of large amounts of CO and at quite low temperatures so that any diffusion process should be slow and strongly hindered.

This dense, mixed and disordered O+CO layer starts to react to CO_2 at surface temperatures around 200 K giving rise to the reaction peak β_3. At very high O/CO ratios, however, this channel is weakened because its specific spatial requirements cannot be met for as many CO molecules without transport. The onset of transport, which will eventually lead to ordering and demixing, then produces reaction peak β_2. The β_2 peak could then correspond to reaction in dense mixed ordered island, similar (in coverage, not necessarily in order) to the (2×1) islands on Pd(111). Indeed, the residual total O+CO coverage before the β_2 peak is still above 0.45 where that peak exists.

On the other hand, the minimum amount of oxygen for the appearance of this peak was found to be between 0.3 and 0.35, which could be connected with the formation of $(\sqrt{3}\times\sqrt{3})R30°$ structures of O and CO, as on Pd(111).[26] If this critical oxygen coverage is not reached, $p(2\times2)$ ordered oxygen islands are formed, and the transport-limited reaction at their boundaries gives rise to the β_1 reaction peak which continuously goes over into reaction in a 2D gas in its tail for low remaining coverages. Under molecular supply from the gas phase, only the conditions for β_1 and its tail are possible.

Partly similar findings as for this system were observed during CO oxidation on Rh(111)[4] for layers prepared in a similar way as ours. Two reaction peaks could be observed and characterized as being due to reactions of mixed disordered layers and, at higher temperatures, reactions out of ordered islands of CO and O. No compression of the $p(2\times2)$ ordered oxygen layer by adsorbed CO was found for this system, possibly because oxygen is more strongly bound on this surface. The close resemblance of the general behavior of this reaction on the (111) surfaces of Pd and Rh, although with some system specific differences in detail, seem to corroborate our assumption that the behavior on Pt(111) is very similar.

B. Reaction dynamics, energetics, and angle-velocity correlations of the various reaction paths

In all the cases of hyperthermal angularly peaked distributions described above, the reaction probability and the distribution of the reaction energy over the various degrees of freedom of this exothermic reaction are governed by a multidimensional potential energy surface. The latter will contain the internal degrees of freedom of the reactants as well as their frustrated rotations and translations, and the same for the product molecule. The activation barrier between reactants and products roughly divides this energy surface into two parts. From our measurements of the translational energies and their angular behavior for the product molecule alone a full exploration of this potential energy surface is not possible, of course. However, the high fraction of total reaction energy appearing in the product translation (see below) and the fact that it does not vary much with surface temperature (except for the very high T_s/low coverage range) show clearly that for these reaction paths equilibration of the product with the heat bath provided by the surface does not occur (except for the Maxwellian part of β_1). This suggests that the shape of the potential energy surface is such that the main acceleration of the product occurs late in the exit channel ("late downhill"). Strongly hyperthermal energy distributions have been found also for the vibrational and rotational degrees of freedom[13,14] as for the translation;[8] the vibrational energy was found to increase with O coverage.[14] It would be expected that the distribution of energy over the coordinates depends strongly on the configuration of the transition state. Indeed, calculations of Kwong *et al.*,[32] using a generalized Langevin formalism and a classical trajectory approach have demonstrated this. We might expect then, that the distributions for the different paths observed here could be quite different. However, an interesting feature of our results is that the translational energy distributions of the β_1 and the α peaks (mean energies and speed ratios, and their angular dependences; see Fig. 6) are the same within our errors, even though the conditions under which they arise are very different in terms of temperature, coverages, and even (overall) reactants. Of course, there could still be very different internal energy contents in the two species, but it is quite improbable that this similarity in the parameters accessible to us is a mere coincidence. A possible explanation would be that, however different the reaction path to the transition complex is, the exit channel is essentially the same. We shall discuss below in context how this could be possible. The equilibrated part of the β_1 peak, on the other hand, might come from an entirely different reaction path going via another transition complex and leading to equilibration directly; or it might arise from an initially similar product, which, due to special circumstances, becomes equilibrated in a secondary interaction.

We will discuss the various species separately as far as possible in view of the still limited information, drawing on other work where possible, and addressing particularly interesting aspects in each case.

1. The fast focused species

a. The β_1^f state. As discussed in Sec. IV A, the species corresponding to this RTPT peak very likely stems from the reaction between O and CO at the boundaries of O islands. In our dense layers such reactions occur already between 300 and 350 K. This interpretation requires the formation of segregated, ordered O islands from dense mixed layers by about 300 K, despite the limited mobility in pure O layers mentioned above. However, this might not be very critical for the actual reaction dynamics. As discussed, connection can be made to the work at lower coverages and higher temperatures. As the stability of O islands extends to very low coverages, as argued above, we expect that basically the same type of reaction was investigated by molecular beam and (our and other) continuous flow experiments carried out at surface temperatures above 550 K. Eventually there will be a dilute 2D gas, and the similarity of results (with only smoothly varying mean energies and activation energies) suggests that the essential local dynamics are the same throughout this range. These measurements of the low coverage regime can be compared with ours, and will be discussed together, therefore. We first review the reaction mechanism for this reaction channel in the limit of small coverages, i.e., for isolated species. The influence of finite CO and O coverages for this reaction path—our RTPD experiments were carried out at remaining O coverages between 0.18 and 0.28—will be considered in a second step.

The strong focusing of the products along the surface normal shows that the transition state possesses a configuration in which a strong force in the surface normal is exerted onto the forming CO_2 species. Intuitively, this might appear easiest for a reaction path in which the CO molecule "climbs" on top of an O_{ad}, finally leading to an essentially upright O–CO complex, as appears to happen for the $N+NO\rightarrow N_2O$ (Ref. 33) and $N+CO\rightarrow NCO$ (Ref.

34) surface reactions. Such a model has been proposed by Matsushima in connection with his observation that the maximum in the angular distribution of CO_2 reactively desorbed from Pt(110), Pd(110), and Ir(110) surfaces is tilted away from the surface normal.[35] Certainly, the electronic rearrangement from a strong O–surface bond to a strong O–CO bond would provide the acceleration of the resulting upright OCO molecule which interacts with the surface very weakly, even much more weakly than the normal CO_2 or CO_2^- species which lie down on the surface; rotational excitation would be induced by the statistical deviations from the straight upright configuration of the transition state, and deviations of the interatomic distances in the latter from those of the final CO_2 molecule would lead to vibrational excitation. Indeed, the mentioned trajectory calculations[32] lead to the conclusion that such a transition complex agrees best with the available information. On the other hand, the transition complex assumed by most of the earlier work (see, e.g., Ref. 2), which consists of a bent O–CO species making contact with the surface via the C and the (incoming) O would correspond best to the intuitive picture of how an O atom would approach an adsorbed CO molecule for reaction, and would lead to a similar picture no matter whether the reacting O atom stems from thermal activation of an O adatom or from (thermal or photoinduced) dissociation of O_2. In the LH case, the activation energy would then mainly be needed to weaken the O–surface bond; the transition complex would possess a C–surface distance roughly like the initial CO admolecule, so that a strong repulsive force perpendicular to the surface would result when the bonding switches from O–surface to O–CO. Again, vibrational and rotational excitations are easily envisaged. A clear decision would obviously require the simultaneous knowledge of all degress of freedom for each well-defined reaction channel which is not available presently.

Our data can be used, however, to estimate the reaction energetics with a simple model with one-dimensional reaction coordinate, as has been used by many authors (see, e.g., Ref. 2). An estimate of the total energy available for the product can be made using the diagram of Fig. 7. We start with the general $CO_{ad}+O_{ad}$ channel. Whereas the adsorption energies of the pure reactants CO (E_{CO}) and oxygen (E_O, referred to gas phase O_2) are well known,[27,36] the activation energy E_{LH}^* can only be determined by explicitly assuming that the reaction $CO_{ad}+O_{ad}\rightarrow CO_2$ is rate limiting. With this assumption $2E_{LH}^*=101$ kJ/mol was obtained in the zero coverage limit, decreasing to 50 kJ/mol at coverages $\Theta_O \geqslant 0.1$.[2] The product energy can then be calculated from $E_P=\Delta H+E_{LH}^*-E_{CO}-E_O$, where $\Delta H=283$ kJ/mol is the energy of formation of free CO_2 from the free molecules CO and O_2. Assuming that the heats of adsorption of CO and O are essentially the same in the coadsorbed layers as in the pure layers the product energy in the low coverage limit can be calculated to be 132 kJ/mol or 1450 meV per molecule. In the coverage ranges considered here the heats of adsorption do not seem to depend strongly on coverage both for CO and oxygen.[27,36] Extending the assumption just made to higher coverages,

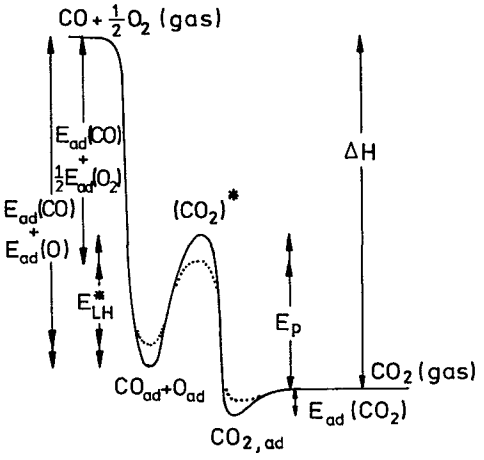

FIG. 7. One-dimensional energy diagram for the CO oxidation on Pt(111) by reaction of adsorbed O and CO (after Ref. 2) and by reaction of adsorbed CO with nascent O produced by dissociation of adsorbed O_2. ΔH is the total enthalpy of reaction; $E_{ad}(CO)$, $E_{ad}(O_2)$, $E_{ad}(CO)$, and $E_{ad}(CO_2)$ are the heats of adsorption for atomic and molecular oxygen, CO and CO_2, respectively, whereas E_{LH}^* represents the activation energy for CO_2 formation, and E_P is the resulting total energy available after reaction on and desorption from the surface. The dotted lines indicate the coverage dependence of the various quantities and, for the adsorption energy of CO_2, the weaker bonding of a possible different configuration.

and neglecting any coverage dependent change in the heats of adsorption of both reactants, the decrease in E_{LH}^* as a function of coverage also decreases E_P by the same amount, so that $E_P=900$ meV is obtained for $\Theta_O \geqslant 0.1$. These values are included in Table II. Of course, if the decrease of activation energy is in part due to a decrease of adsorption energies, then the decrease of product energy is smaller. Our values for the translational energy at low and intermediate coverages obtained in the steady-state experiments, 600 and 440 meV, then correspond to between 40% and 50% of the available energy. At higher coverages, the translational energies decrease further, as seen in Table II, which would suggest a stabilization of the transition complex or a smaller share of translation.

In order to estimate the partitioning among the other degrees of freedom of the product energy we draw on the measurements carried out with chemoluminescence at surface temperatures between 730 and 900 K, i.e., at low coverages.[13,14] In particular, the last work was carried out under essentially collision-free conditions, for $\Theta_O=0.1$ and very low Θ_{CO} at 810 K; in qualitative agreement with the other results, effective rotational temperatures of 1000 K and vibrational temperatures between 1500 and 2500 K (depending on the vibrational mode) were found. This corresponds to about 380 meV per CO_2 molecule of internal energy, i.e., an amount comparable to the translational energy, if we assume that the value appropriate for these conditions lies between our lower steady-state value and the β_1 value. For an expected total product energy of 900 meV, only about 20% of the total product energy is transferred into the substrate. This estimate also relies on the assumption that no internal excitations are contained in the activated complex of CO_2^* and the rovibronic excita-

tions measured are fully due to this partitioning of the product energy.

The assumption that the same underlying mechanism is effective for surface temperatures between 330 and 800 K, is made plausible by the comparison of our steady state measurements with molecular beam results. Differences observed in the experimental results can be best ascribed to simple differences in coverage, in particular that of oxygen. At 800 K we obtained an average translational energy of 600 meV per molecule in the continuous flow experiment, in quantitative agreement with older molecular beam data[8] obtained under similar conditions. Our TPD data yielded 330 meV at $T_s=350$ K. The values obtained in our continuous flow experiments at lower temperatures lie in between, in qualitative agreement with the very recent molecular beam data of Hoinkes *et al.*[11] who obtained 400 meV at $T_s=550$ K. Because of the essential decoupling of the product from the heat bath of the surface, these differences cannot be caused directly by the surface temperature. Rather they are best explained as a simple coverage effect. For the extreme low coverage limit corresponding to the measurements at 800 K we estimated the product energy to 1450 meV per molecule while for an oxygen coverage $\geqslant 0.1$ we arrived at 900 meV. It is seen that the increase in translational energy when going from 330 to 800 K corresponds very well to the increase of product energy, i.e., the same percentage of about 40% of the product energy is found as translational energy in both cases. Since it is likely that the fraction dumped into the solid is roughly constant, too, we assume that also the rovibrational fraction is roughly the same. No contradiction against the assumption of an essentially identical reaction path throughout this coverage and temperature range is thus found.

b. The β_2 and β_3 peaks. There is no obvious reason why the atomistic path of reaction should be very different for the reaction at high concentrations of both reactants which constitute TPD peaks β_2 and β_3, except that there could be some spatial restriction on the transition complex. For instance, if a variety of pathways corresponding to the various angular arrangements of the transition state should exist, the crowding on the surface could select that with the smallest lateral extent. This would be the roughly linear, upright species. In terms of the previous considerations for the β_1 species, coverage dependent energetic as well as kinetic modifications of both the transition state and of the activation barrier between adsorbed species and transition state are expected, again. Indeed, the translational energy found for these desorption peaks is lower than for β_1^f. Because of the mode of formation of these high density layers, we have argued that the reaction proceeds in dense mixed O+CO layers or boundaries, respectively. While this will increase the density of transition states and thus the overall reaction rate, it should not strongly influence the atomistics of reaction, unless the transition state itself is influenced. The fact that the translational energies are clearly lower here could be taken as an indication for such a change; another possibility would be that because of the high density of adsorbates, energy is transferred from the outgoing molecule to neighbors.

A second interesting point is the finding that here the lowest average translational energies (among the fast species) are correlated with the narrowest angular distributions. It contradicts a general rule saying that the more (normal) energy is channelled into the products the narrower is the angular distribution. Again this could be due to the high adsorbate density for these reaction conditions which can be active in two ways. First, it can induce focusing of the leaving product molecules by repulsive interactions with neighbors, restricting their paths through scattering; the scattering processes can be partly inelastic thereby reducing the translational energy of the leaving CO_2 molecule, as just suggested. Second, the high density will strongly restrict lateral mobility, and even frustrated translations and rotations of the reactant molecules. Less lateral momentum will then be contained in the transition state. This sharpens the angular distributions. If this second process is important, one would expect decreased rotational excitations of the product whereas vibrations should not be influenced much. The possible restriction to a "standing-up" transition complex could in fact be considered as an extreme of this influence. The difference between β_2 and β_3, with their different angular focussing, probably consists of different local environments which cannot be discussed further on the basis of the available data; again structural data would be very valuable.

c. The α peak. A completely different path could be expected in principle for the α peak. Direct reaction between O_2 and CO leading to $O_{ad}+CO_2$ appears extremely unlikely. Rather, as discussed all previous and present information about it suggests that it is due to reaction of CO with O atoms from the dissociation of O_2 which can proceed because in the temperature range concerned oxygen molecules desorb, making space for dissociation if necessary. The ease with which the reaction occurs shows that no activation of O is necessary for α, i.e., that the oxygen atoms formed by O_2 dissociation must react before they become settled into the surface. This is corroborated by inspection of the energetics. As shown in Fig. 7, the energy level of a forming O plus an adsorbed CO is just about the same as that estimated for the (O+CO)-derived transition complex. It is not clear from our data whether this means that the O atom reacts as it is formed ("nascent"O; see also Ref. 16), or whether it is merely not yet translationally fully accommodated ("hot"O). The very high total adsorbate density, which should lead to very fast accommodation by multiple collisions, would argue against the second possibility; therefore we prefer the picture of a nascent reacting O. In any case, if we define a LH reaction as one due to reaction between fully accommodated surface species with activation by thermal fluctuations, then either of these would be non-LH reactions.

Furthermore, it is difficult to conceive that the very similar translational energy distributions and angular variation of β_1^f and α are a mere coincidence. As mentioned above, this finding could mean that the transition complex and its outgoing channel are essentially the same for these two species, and that they only differ in the way how it is reached. This is again consistent with the energetics shown

in Fig. 7, if for α about the same percentage of the total product energy appears as translation of the CO_2 product as for β_1^f. As to a possible chemical picture of how this could come about, this is most easily conceived for a transition complex making surface contact via the C end of CO and the approaching O. To enter this state, an *adsorbed* O atom has to be essentially lifted out of its surface bond, explaining the necessary activation energy; the same state could be accessible directly by a *nascent* or *hot* O atom, in agreement with our energetic picture. Of course we cannot exclude that all these agreements are coincidental and a different product energy is canceled by strongly differing branching into the internal modes; but such a fortuitous canceling would appear quite improbable. A measurement of the internal mode distribution for this species would be highly desirable. The fact that focusing is much smaller for α than for β_2 and β_3 although the adsorbate density is the highest on average might be due to the empty space produced locally by the dissociation of the (lying-down) oxygen molecule which is likely preceded by the desorption of another O_2 molecule.

2. The accommodated species

The findings on the fully accommodated β_1^s peak, which is so obvious in our TPD results, are a bit controversial in the literature. Older measurements carried out with molecular beams at $T_s = 800$ K,[8] i.e., for very small concentrations of both O and CO, were not able to detect the corresponding bimodality in the product flux. Indeed, our continuous flow experiments using essentially the same conditions of temperature and partial pressures also found that the fully accommodated component continuously decreases as a function of increasing surface temperature and reaches the limit of detectability at $T_s = 800$ K. On the other hand, the very recent molecular beam work of Hoinkes *et al.*[11] detected it at $T_s = 550$ K. They do not give the oxygen coverage, which might be important, but mentioned that they searched for optimal conditions, in particular with respect to the angle of incidence of the O_2 beam. Segner *et al.*[9] who investigated earlier the bimodal partitioning in detail by measurements of the angular distributions only found that the cosine fraction decreased with *increasing* coverages of CO and O, and with increasing surface temperature. These authors also showed that it increased with increasing step density on the surface.

Before we discuss its probable origin, we consider the question whether the data really have to be explained by *two* contributions only. This question has been raised by Brown and Sibener[5] who for Rh(111) found a broad distribution which could not be fit bimodally, and who stressed the point that there is no reason to expect $\sim\cos^n \vartheta$ distributions. However, *both* our angle and (angle-dependent) energy distribution data are fit excellently with two contributions, of which in both cases one is a Maxwellian and the other possesses a distribution with constant n value similar to those seen in the other cases where *no* Maxwellian contribution exists. Therefore we believe that in this case there *are* two separable contributions. This at the same time argues against a continuous variation of interaction, whereby the outgoing β_1 species would statistically lose some energy to become fully accommodated in the extreme. In such a case a continuous distribution would indeed be expected.

While the existence of this separate component is now clear, the mechanism of its formation is not. A dominating influence of steps for it was postulated by Segner *et al.*[9] on the basis of their mentioned finding. This could be understood if the outgoing molecules suffer multiple inelastic scattering at steps before they escape from the surface. From the efficiency of this process derived from known step densities in Ref. 9 we can safely exclude this explanation as the main source for β_1^s formation as our defect density was less than 1%, but up to two thirds of the total desorption flux was contained in peak β_1^s. Another conceivable explanation would be that thermally generated defects (Pt adatoms and vacancies) are responsible for β_1^s instead of static defects. This possibility can also be ruled out, not only because a huge cross section for inelastic scattering must be assumed at the low defect concentrations that can be thermally generated at surface temperatures of 350 K, but in particular because the fraction of β_1^s should then increase with increasing surface temperature contrary to our findings. We therefore conclude that the β_1^s species observed here must be due to an intrinsic property of the flat surface. Also the above discussion of the question of clear separability suggests that indeed the accommodated species comes about by a different reaction channel, and not simply by some secondary scattering, since then one should expect continuous variations.

We therefore conclude that the β_1^s channel comes about by a reaction path intrinsically different from that of β_1^f. While the available data are not sufficient to give an unequivocal explanation, we venture a speculative explanation to induce further work. Neither of the transition state configurations discussed above corresponds to the optimally bound CO_2 adspecies. Calculations for CO_2 on Ni (Ref. 37) indicate that there are two stable orientations of CO_2 on transition metals which are both essentially lying down on the surface, a species bound via C and one O and another one bound via both O ends, the latter being more strongly bound and closer to CO_2^-. If this is qualitatively correct also for the Pt surface, one could indeed envisage two types of transition states. One would be closer to the first species, but with a too short C–metal bond length; its stretched upright extreme could be induced by the spatial restrictions in the β_2 case. The other one would be closer to the ionic species and more strongly bound. Because of the lack of a C–metal bond, the main energy liberated in CO_2 formation in the latter case could be directed parallel to the surface and would therefore be easily transferred to coadsorbates and ultimately to the surface. Steps and other defects would help this transfer, explaining the findings of Ref. 9. For sufficient trapping times, internal energy could also be transferred to the surface before desorption. The temperature dependence of the trapping time for this species would explain the observed decrease of this channel with temperature, since at sufficiently high temperature this channel would be wiped out thermally. Binding ener-

gies of the order of 15 kJ/mol would suffice to explain the observations. The observed influence of oxygen coverage could be a coadsorbate destabilization effect or an effect of spatial requirements. These speculative considerations might induce further, in particular theoretical work.

V. SUMMARY

Reactive thermal desorption (RTPD) of CO_2 product molecules from the oxidation reaction $CO+O \rightarrow CO_2$ has been studied starting with mixed layers of CO and molecular oxygen, up to very high initial coverages. Four reactively produced CO_2 peaks are observed. For the β_1 peak these results have been compared with continuous flow reactions at surface temperatures between 420 and 800 K. These results are comparable to those of RTPD in its high temperature, medium to low coverage range, if the corresponding coverages of atomic oxygen are taken into account.

The four reaction peaks observed during RTPD all show strongly nonthermal energy distributions, i.e., the average translational energy exceeds by far a value of $2\ kT_s$, and the measured velocity distributions are narrower than Maxwell–Boltzmann distributions (which shows up in normalized speed ratios <1). Only the peak β_1 contains a contribution which is thermally fully accommodated to the surface. Whereas this part of the desorption flux shows a $\cos\vartheta$ angular distribution, all others are much more strongly peaked. The latter, which contain most of the total desorption flux (between 75% and 95%), are obviously not accommodated to the surface, and carry away a considerable fraction of the product energy as translational energy. For the β_1 peak we estimate this fraction to be approximately 40%.

We interpret the occurrence of mainly nonaccommodated product species as due to formation of a transition complex with strong repulsion from the surface for *all* nonaccommodated reaction peaks on the surface, and the formation of the transition state as rate limiting. Therefore once formed, the CO_2 molecule is accelerated away from the surface. It seems likely that the main partitioning of the product energy occurs during this last step.

The rate of formation of CO_2^* is found to be strongly influenced by the density as well as by the structural configuration of the reactants on the surface. Changes in average interadsorbate distance might be the main reason for changes of the activation energy for the transition state and of the binding energy of the reactants because of lateral interactions which cause corresponding changes of the product energy E_P. Both modify strongly the reaction rates because the reaction probability is strongly influenced by mobility for a large part of our experimental conditions: On the one hand, frozen-in mixing of the reactants and favorable relative configurations enhance the reactivity and lead to high rates at quite low temperatures; on the other, demixing due to the tendency of both reactants to form separated islands slows down the reactivity when mobility sets in.

Our results are consistent with the assumption that basically the same type of reaction, but modified by different local configurations, is effective in the formation of product peaks β_1^f, β_2, and β_3; for peak α it appears likely that the reaction of unaccommodated (nascent or hot) O atoms from O_2 dissociation leads to essentially the same transition state as for β_1^f as far as the exit channel is concerned. The smaller translational energy and the narrower angular distributions of peaks β_2 and β_3 may be due to scattering of the product molecules at their neighbors in dense mixed layers of CO and O, but a restriction on the orientation of the transition complex by the close neighbors appears also possible.

The accommodated peak β_1^s, on the other hand, which appears only at low surface concentrations of CO, but not of O, and vanishes at high temperatures, might be due to a basically different type of transition state. A more ionic species with essentially flat lying configuration and stronger surface bond would greatly enhance the probability of collision with other adatoms and with defects, and might have the necessary trapping times to explain the observed equilibration; it seems plausible, therefore, but should be further scrutinized.

Summing up, we have investigated the oxidation of CO on Pt(111) in coadsorbed layers of high density. Under these strongly non-equilibrium conditions of the initial layers, the reaction rates seem to be strongly influenced by the local configurations of CO and O on the surface. The dynamics of the reaction, on the other hand, can be similar—as concerns the exit channel—for very different reaction conditions (β_1^f and α) but also very different for identical reaction conditions (β_1^f and β_1^s).

ACKNOWLEDGMENTS

We thank Sabine Müller for her participation in the steady state measurements. This work was supported by the Deutsche Forschungsgemeinschaft through SFB 338.

[1] T. Engel and G. Ertl, Adv. Catalysis **28**, 1 (1979); T. Engel and G. Ertl, in *The Chemical Physics of Solid Surfaces and Heterogeneous Catalysis*, Vol. 4, edited by D. A. King and D. P. Woodruff (Elsevier, New York, 1982).
[2] C. T. Campbell, G. Ertl, H. Kuipers, and J. Segner, J. Chem. Phys. **73**, 5862 (1980).
[3] J. L. Gland and E. B. Kollin, J. Chem. Phys. **78**, 963 (1983).
[4] T. Matsushima, T. Matsui, and M. Hashimoto, J. Chem. Phys. **81**, 5151 (1984).
[5] L. S. Brown and S. J. Sibener, J. Chem. Phys. **89**, 1163 (1988); **90**, 2807 (1989).
[6] T. Engel and G. Ertl, J. Chem. Phys. **69**, 1267 (1978).
[7] R. L. Palmer and J. N. Smith, Jr., J. Chem. Phys. **60**, 1453 (1974).
[8] C. A. Becker, J. P. Cowin, L. Wharton, and D. J. Auerbach, J. Chem. Phys. **67**, 3394 (1977).
[9] J. Segner, C. T. Campbell, G. Doyen, and G. Ertl, Surf. Sci. **138**, 505 (1984).
[10] T. Matsushima, Surf. Sci. **127**, 403 (1983).
[11] E. Pöhlmann, M. Schmitt, H. Hoinkes, and H. Wilsch, Surf. Sci. **287/288**, 269 (1993).
[12] T. Matsushima, Y. Ohno, and J.-I. Murakami, Surf. Sci. **287/288**, 192 (1993).
[13] D. A. Mantell, S. B. Ryali, B. L. Halpern, G. L. Haller, and J. B. Fenn, Chem. Phys. Lett. **81**, 185 (1981); S. L. Bernasek and S. R. Leone, *ibid.* **84**, 401 (1981); D. A. Mantell, S. B. Ryali, and G. L. Haller, *ibid.* **102**, 37 (1983); M. Kori and B. L. Halpern, *ibid.* **110**, 223 (1984); L. S. Brown and S. L. Bernasek, J. Chem. Phys. **82**, 2110 (1985); D. A. Mantell, K. Kunimori, S. B. Ryali, G. L. Haller, and J. B. Fenn, Surf.

Sci. **172**, 281 (1986); K. Kunimori, H. Uetsuka, T. Iwade, T. Watanabe, and S. Ito, *ibid.* **283**, 58 (1993).
[14]G. W. Coulston and G. L. Haller, J. Chem. Phys. **95**, 6932 (1991).
[15]C. T. Rettner and C. B. Mullins, J. Chem. Phys. **94**, 1626 (1991).
[16]C. B. Mullins, C. T. Rettner, and D. J. Auerbach, J. Chem. Phys. **95**, 8649 (1991).
[17]W. D. Mieher and W. Ho, J. Chem. Phys. **91**, 2755 (1989).
[18]K.-H. Allers, H. Pfnür, P. Feulner, and D. Menzel, Surf. Sci. **291**, 167 (1993).
[19]K. H. Allers, H. Pfnür, P. Feulner, and D. Menzel, Surf. Sci. **286**, 297 (1993).
[20]E. Kellner, German Patent No. P 2451717.1, U. S. Patent No. 4,089,185.
[21]H. Schlichting and D. Menzel, Surf. Sci. **285**, 209 (1993).
[22]A. C. Luntz, J. Grimblot, and D. E. Fowler, Phys. Rev. B **39**, 12903 (1989); A. C. Luntz, M. D. Williams, and D. S. Bethune, J. Chem. Phys. **89**, 4381 (1988).
[23]K.-H. Allers, H. Pfnür, P. Feulner, and D. Menzel (in preparation).
[24]J. L. Gland, B. A. Sexton, and G. B. Fisher, Surf. Sci. **95**, 587 (1980).
[25]S. Akhther and J. M. White, Surf. Sci. **171**, 527 (1986).
[26]T. Matsushima and H. Asada, J. Chem. Phys. **85**, 1, 658 (1986).
[27]G. N. Derry and P. N. Ross, J. Chem. Phys. **82**, 27, 72 (1985).
[28]H. Conrad, G. Ertl, J. Küppers, and E. E. Latta, Surf. Sci. **65**, 245 (1977).
[29]C. T. Campbell, G. Ertl, H. Kuipers, and J. Segner, Surf. Sci. **107**, 207 (1981).
[30]G. Ertl and J. Koch, Z. Naturforsch. Teil A **25**, 1906 (1970).
[31]H. Conrad, G. Ertl, and J. Küppers, Surf. Sci **76**, 323 (1978).
[32]D. W. J. Kwong, N. DeLeon, and G. L. Haller, Chem. Phys. Lett. **144**, 533 (1988).
[33]H. J. Kreuzer and L. C. Wang, J. Phys. (Paris) **50**, C8-53 (1989).
[34]K. L. Kostov, H. Rauscher and D. Menzel, Surf. Sci. **287/288**, 283 (1993); R. L. C. Wang and H. J. Kreuzer, Chem. Phys. **177**, 453 (1993).
[35]T. Matsushima, J. Chem. Phys. **91**, 5722 (1989).
[36]G. Ertl, M. Neumann, and K. M. Streit, Surf. Sci. **64**, 393 (1977).
[37]H.-J. Freund and R. P. Messmer, Surf. Sci. **172**, 1 (1986).